Eur Spine J (2016) 25:517–525
DOI 10.1007/s00586-015-4108-6

ORIGINAL ARTICLE

Comparison of the scoliosis curve patterns and MRI syrinx cord characteristics of idiopathic syringomyelia versus Chiari I malformation

Zezhang Zhu[1,2] · Shifu Sha[1,2] · Winnie C. C. Chu[2,3] · Huang Yan[1,2] · Dingding Xie[1,2] · Zhen Liu[1,2] · Xu Sun[1,2] · Weiguo Zhu[1,2] · Jack C. Y. Cheng[2] · Yong Qiu[1,2]

Received: 17 March 2015 / Revised: 1 July 2015 / Accepted: 1 July 2015 / Published online: 11 July 2015

Abstract

Purpose Although the more readily available MR imaging has brought about more incidental findings of idiopathic syringomyelia (IS), no published study has specifically addressed the clinical and imaging features of IS-associated scoliosis. Since IS and Chiari I malformation (CMI)-type syringomyelia are hypothesized to share a common underlying developmental pathomechanism, this study aimed to investigate the scoliosis curve patterns and MRI syrinx cord characteristics of patients with IS comparing with those seen in CMI.

Methods Sixty-one patients with scoliosis secondary to IS were identified and reviewed retrospectively. The curve pattern and specific curve features were recorded and compared with historic CMI controls. Location, size, and morphological appearance of the syrinx were systematically assessed on MR images.

Results The maximal syrinx/cord ratio and rostrocaudal length of the syrinx in IS averaged 0.43 ± 0.16 (range 0.17–0.78) and 4.6 ± 2.5 (range 2–15) vertebral levels, respectively, both of which were smaller than those reported in CMI-type syringomyelia. Regarding the characteristics of IS-related scoliosis, sagittal profiles as well as the frequency of curve patterns and atypical features were all found to resemble those in patients with CMI ($P > .05$). Among the 47 individuals with a single thoracic curve, Fisher exact test revealed a significant correlation between curve convexity and the dominant side of deviated syrinx (83.3 % concordance rate, $P = .021$). In addition, apex of the thoracic curve trended toward being significantly correlated with the level of maximum expansion of the syrinx ($P = .066$).

Conclusions Radiological characteristics of scoliosis were found to be similar between idiopathic and CMI-type syrinx in both the coronal and sagittal planes, adding further evidence to the concept that these entities may be part of a spectrum of disease sharing a common pathophysiological mechanism. The thoracic spine in IS patients tended to be convex to the deviated side of syrinx, which indirectly supported the likely role of spinal cord dysfunction in the pathogenesis of syrinx-associated spinal deformities.

Keywords Idiopathic syringomyelia · Chiari I malformation · Scoliosis · Imaging feature · Coronal asymmetry

S. Sha and Z. Zhu contributed equally to this work.

✉ Yong Qiu
scoliosis2002@sina.com

Jack C. Y. Cheng
jackcheng@cuhk.edu.hk

[1] Department of Spine Surgery, The Affiliated Drum Tower Hospital of Nanjing University Medical School, Zhongshan Road No. 321, Nanjing 210008, China

[2] Joint Scoliosis Research Center of the Chinese University of Hong Kong and Nanjing University, Nanjing, China

[3] Department of Orthopaedics and Traumatology, The Chinese University of Hong Kong, 5/F, Clinical Science Building, Shatin, NT, Hong Kong, China

Introduction

Syringomyelia is an etiologically diverse affliction characterized by a longitudinally oriented fluid-containing cavity that anatomically lies within the spinal cord parenchyma. Whereas syrinx is frequently associated with a Chiari I malformation (CMI) [1], it occasionally occurs

without any readily identifiably causes and hence, the term "idiopathic syringomyelia" (IS) was coined to denote such a unique pathological entity. Over the past several decades, the more readily available MR imaging has brought about more incidental findings of IS, particularly in patients seeking spinal care for the concomitant scoliosis [2, 3].

Syringomyelia presenting with scoliosis as the primary complaint represents a diagnosis which, if unidentified, may lead to a delay in appropriate management. Compared to patients with CMI-related syringomyelia, IS patients in general have less extensive syringes as well as less severe associated neurologic signs and symptoms [4], which, to some extent, renders surgeons less likely to be alerted to the presence of the intraspinal anomaly. Lately, the radiographic features in scoliosis secondary to CMI and syringomyelia have received extensive investigation [5–7], showing left thoracic curve and the absence of apical hypokyphosis as typical traits warranting high index of suspicion for an underlying neural axis abnormality. Thus far, however, no published study has specifically addressed the clinical and imaging features of IS-associated scoliosis. Given the assumption that IS and CMI-type syringomyelia may share a common underlying developmental pathomechanism [4], we sought to determine whether the curve patterns and radiological MRI syrinx cord characteristics of scoliosis secondary to IS resemble those observed in CMI-associated scoliosis.

In addition, as an asymmetrically expanding syrinx is reckoned to cause unilateral damage to the anterior horn that innervates paraspinal musculature and thereby predispose to scoliosis [8, 9], a multitude of investigators have attempted to dissect the correlation between curve direction and deviation of the syrinx [10–12]. Due, in part, to the limited sample sizes and in particular the lack of clearly recorded convex side of double major curves, however, no conclusive evidence has hitherto been obtained. More importantly, taking into account the high incidence of asymmetrical cerebellar tonsillar ectopia as documented in the literature [10, 13], such correlation may potentially be subject to the influence of the laterality of downward displaced tonsils as well. In this regard, the absence of classic foramen magnum pathology in patients with IS allows an accurate and somewhat more unbiased assessment of the relationship between curve direction and syrinx deviation, hence making possible a better understanding of the mechanism by which syringomyelia leads to spinal deformity. As single thoracic scoliosis is the predominant curve type observed in IS [12], we focused on this group of patients in the subset analysis to quantitatively evaluate the correlation of the coronal asymmetries between scoliosis and syrinx.

Subjects and methods

The institutional review board waived the requirement for informed consent for our retrospective review of patient records and images, in compliance with Health Insurance Portability and Accountability Act guidelines.

Patient population

A total of 65 patients referred to our center for evaluation of scoliosis secondary to IS between 1998 and 2011 were identified and reviewed retrospectively. In line with the criteria defined previously [2, 3], diagnosis of IS was made only after ruling out all the known precipitating causes of syringomyelia (CMI, spinal cord tumor, trauma, CNS infection, tethered cord, hydrocephalus, etc.). In addition, patients with a history of spinal surgery, or with syrinx diameter less than 1 mm or syrinx length less than two vertebral levels were excluded from the study.

Clinical and radiographic evaluation

Routine demographic variables including gender and age were collected for each patient as well as information on presenting neurological signs and symptoms. Severity of neurological deficit was determined on the basis of each patient's KPS score [14], and those with a score of 85–100, 65–84 and <65 were classified, respectively, as mild, moderate and severe neurological deficit [15].

The location, size, sidedness, and morphological appearance of the syrinx were systematically evaluated on MR imaging studies. Midsagittal images of the brain and spine were used to assess the rostrocaudal extent of the syrinx, recorded as the number of vertebral segments traversed [6]. The maximal syrinx/cord (S/C) ratio, defined as the anteroposterior diameter of the syrinx divided by the diameter of the spinal cord at the level of maximum expansion, was assessed on transverse MR images to determine the axial width of the syrinx [16]. In addition, syrinx configuration was categorized into slender, circumscribed, moniliform and distended types (Fig. 1), as previously described by Ono et al. [13]. On transverse images, the sidedness of syrinx was identified by measuring the distances between the center of the syrinx and the bilateral rims of the spinal cord [10], and a syrinx with a deviation rate [calculated as (right-side distance at the upper end + right-side distance at the lower end)/(left-side distance at the upper end + left-side distance at the lower end)] of more than 1.10 or less than 0.90 was defined as being eccentrically located [10].

Scoliosis-related indices including primary curve magnitude, curve pattern, and apical, proximal and distal Cobb

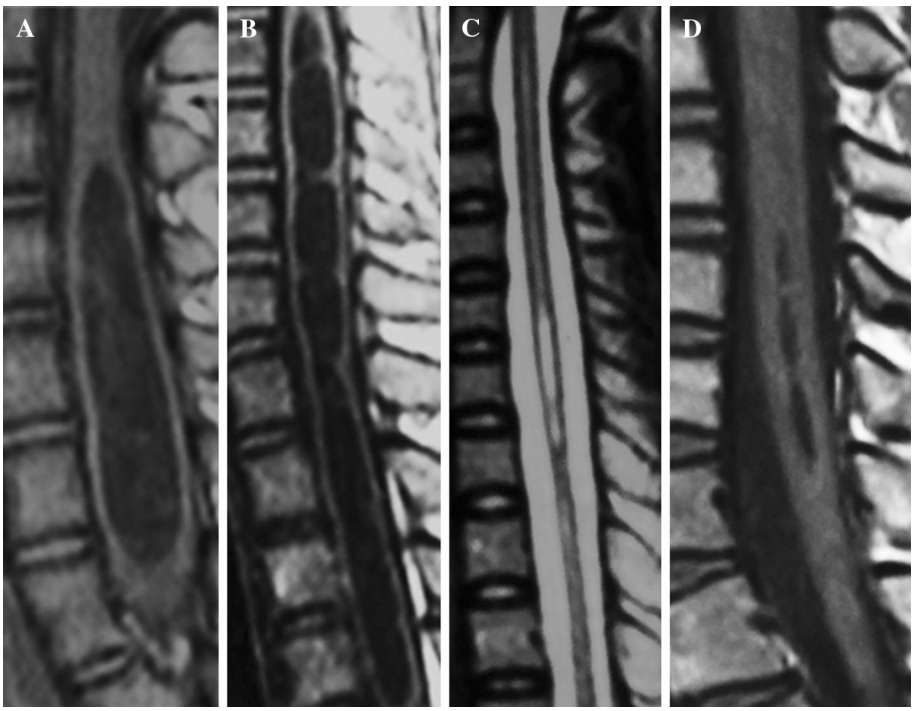

Fig. 1 Configuration of the syrinx. **a** Distended type. **b** Moniliform type. **c** Slender type. **d** Circumscribed type

end vertebrae were analyzed on long-cassette standing posteroanterior radiographs. Coronal plane curve types were classified as thoracic, thoracolumbar/lumbar, double thoracic, or double major curves according to the location of the apices and the curve magnitude. Standing lateral radiographs were also reviewed to quantify thoracic kyphosis (T3–T12) and lumbar lordosis (T12–S1) [5, 6], and values were interpreted with respect to normative data for sagittal profiles in asymptomatic adolescents and adults [17–19]. Specifically, thoracic alignment was defined as hyperkyphotic (>50°), normal (20°–50°), and hypokyphotic (<20°), and accordingly, lumbar alignment was defined as normal (54°–74°), hyperlordotic (>74°), and hypolordotic (<54°) [5, 6]. According to the Spiegel classification scheme [5], atypical coronal curve patterns included left thoracic, left thoracic/right lumbar, left thoracic/right thoracolumbar, right and left double thoracic, right thoracic (King IV), and triple and quadruple curve patterns. "Typical" patterns would therefore consist of right thoracic, right thoracic/left lumbar, right thoracic/left thoracolumbar, thoracolumbar, and lumbar curve patterns.

All measurements were performed independently by two members of the study group (S.S. and H.Y.). Differences were resolved via discussion between the two, with a senior spine surgeon (Z.Z.) being consulted if disagreement persisted. Since curve patterns of scoliosis associated with CMI-type syringomyelia are well documented in the literature in both the coronal and sagittal planes, historical series (including a big series from our center) [5, 6] were used as controls for comparison.

Statistical analysis

Data analyses were performed using SPSS version 19.0 (SPSS Inc., Chicago, IL). Distributions of variables are presented as mean ± standard deviation (range). Differences between measures were assessed by means of the Student *t* test and Wilcoxon rank test, depending on the parametric qualities of the variable analyzed, for a significance level of <.05.

Results

Patient characteristics

A total of 61 patients including 32 males and 29 females were ultimately enrolled into this study. The age at presentation ranged from 10 to 21 years, with a mean of 15.5 years. Neurological deficits were detected in 21 cases (34.4 %) on the initial clinical examinations and classified as mild in 14 (23.0 %), moderate in 5 (8.2 %), and severe in 2 (3.3 %) according to the KPS grading system. Presenting symptoms included extremity or back pain in 12 patients (19.7 %).

Radiological features of IS

The maximal S/C ratio and rostrocaudal length of the syrinx averaged 0.43 ± 0.16 (range 0.17–0.78) and 4.6 ± 2.5 (range 2–15) vertebral levels, respectively, both of which were smaller than those observed in prior CMI-type syringomyelia cohorts (Table 1).

The proximal syrinx level ranged from C2 to T4, while the distal level varied from C4 to T10. Distribution of syrinx included 28 (45.9 %) lesions isolated to the cervical spine, 28 (45.9 %) crossing the cervicothoracic junction, and a further 5 (8.2 %) involving the thoracic cord only. Syrinx configuration was classified as circumscribed type in 40 patients, slender in 14, moniliform in 2, and distended type in 5. Concerning the syrinx morphology on the coronal plane, centrally located cavity was found in 40 (65.6 %) cases, with left and right deviation presenting in 11 (18.0 %) and 10 (16.4 %), respectively. All the above parameters were further evaluated with respect to age and gender; no significant difference, however, was noted between males and females, or between adolescents (10–18 years) and adults (>18 years) in terms of either variable ($P > .05$; Table 2).

Radiographic features of scoliosis

Curve types of the scoliosis included 47 single (28 right and 19 left) thoracic, 3 double thoracic, 8 double major, and 3 thoracolumbar curves. Based on the classification scheme proposed by Spiegel et al. [5], 25 (41.0 %) patients were identified as having atypical curve patterns. In the 36 patients with "typical" coronal patterns, a superior/inferior shift of the apex or the upper/lower end vertebrae was considered as atypical feature [5, 6], and 27 (75.0 %) cases fell into this category. On the sagittal plane, the thoracic kyphosis averaged 46.0° ± 19.8° (range 5°–110°) for the entire dataset, with thoracic hyperkyphosis and hypokyphosis being demonstrated in 22 (36.1 %; Fig. 2) and 3 (4.9 %) cases, respectively. As for the lumbar lordosis (mean 57.8°; range 20°–88°), 42.6 % of patients were within the normal range versus 42.6 % hypolordotic and 14.8 % hyperlordotic. Comparing these data with published results for scoliosis associated with CMI-type syrinx, no significant difference was found in the distribution of coronal curve patterns, sagittal profiles, or the frequency of atypical features ($P > .05$; Table 3).

Relationship between syrinx and spinal deformity characteristics

The primary coronal curve magnitude (71.8° ± 31.5°, on average) was not related to the maximal S/C ratio or syrinx length ($P > .05$), whereas a significant correlation was observed between the two latter variables (Spearman correlation test, $r = 0.266$; $P = .038$). In regard to the location of syrinx relative to scoliosis, the level of maximum expansion of the syrinx trended toward being significantly correlated with apex of the thoracic curve (Fisher exact test, $P = .066$). In addition, the syrinx (i.e., maximal S/C ratio and syrinx length) and curve sizes did not differ significantly between symptomatic and asymptomatic patients (Wilcoxon rank test, $P > .05$), or between patients with different severities of neurological deficits (in terms of none, mild, moderate, and severe; Kruskal–Wallis test, $P > .05$).

The correlation between the side of syrinx deviation and convex side of the scoliosis was investigated in the 47 patients with a single thoracic curve. Among the 18 individuals in whom the syrinx was eccentrically located, an 83.3 % concordance rate was found in the laterality between curve convexity and the syrinx (Fisher exact test, $P = .021$; Table 4).

Discussion

The idiopathic form of syringomyelia classically does not have an anatomical abnormality readily seen on regular imaging. Multiple lines of evidence, however, demonstrates that these patients may harbor "Chiari-like" properties such as increased peak cerebrospinal fluid flow velocities [20, 21], steeper tapering of the upper cervical spinal canal [22] and underdeveloped osseous posterior fossa accompanied by a craniocerebral disproportion [4, 23]. Suboccipital decompression, a neurosurgical technique widely adopted for treatment of CMI, has also been proved to be effective for symptomatic IS in terms of diminishing syrinx size and arresting symptom deterioration [4, 24, 25].

Table 1 Comparison of syrinx dimensions between idiopathic and Chiari I-type syringomyelia

	Idiopathic syringomyelia	Chiari I-type syringomyelia		
	Present study	Wu et al. [29]	Zhu et al. [30]	Ono et al. [13]
Sample size	61	44	54	42
Age (years)	15.5	12.1	10.2	44.8
Maximal syrinx/cord ratio	0.43	0.61	0.52	–
Syrinx length (vertebrae)	4.6	8.1	10.0	12.9

Table 2 Evaluation of idiopathic syrinx with respect to age and gender

Variable	Gender			Age		
	Males	Females	*P*	Adolescents	Adults	*P*
No.	32	29		48	13	
Maximal syrinx/cord ratio	0.43 ± 0.15	0.42 ± 0.17	NS†	0.43 ± 0.17	0.40 ± 0.13	NS†
Length (vertebrae)	5.3 ± 2.8	3.7 ± 1.8	NS†	4.5 ± 2.2	4.9 ± 3.5	NS†
Location						
Proximal level	C2–T2	C2–T4	NS	C2–T4	C2–T3	NS
Distal level	C6–T10	C4–T7		C6–T7	C5–T10	
Configuration						
Circumscribed	20 (62.5 %)	20 (69.0 %)	NS	31 (64.6 %)	9 (69.2 %)	NS
Slender	8 (25.0 %)	6 (20.7 %)		11 (22.9 %)	3 (23.1 %)	
Moniliform	2 (6.25 %)	0		1 (2.1 %)	1 (7.7 %)	
Distended	2 (6.25 %)	3 (10.3 %)		5 (10.4 %)	0	
Syrinx deviation						
Center	21 (65.6 %)	19 (65.6 %)	NS	33 (68.8 %)	7 (53.8 %)	NS
Left	6 (18.8 %)	5 (17.2 %)		8 (16.7 %)	3 (23.1 %)	
Right	5 (15.6 %)	5 (17.2 %)		7 (14.6 %)	3 (23.1 %)	

NS statistical non-significance ($P > .05$)

† Wilcoxon rank test, otherwise the Fisher exact test was used

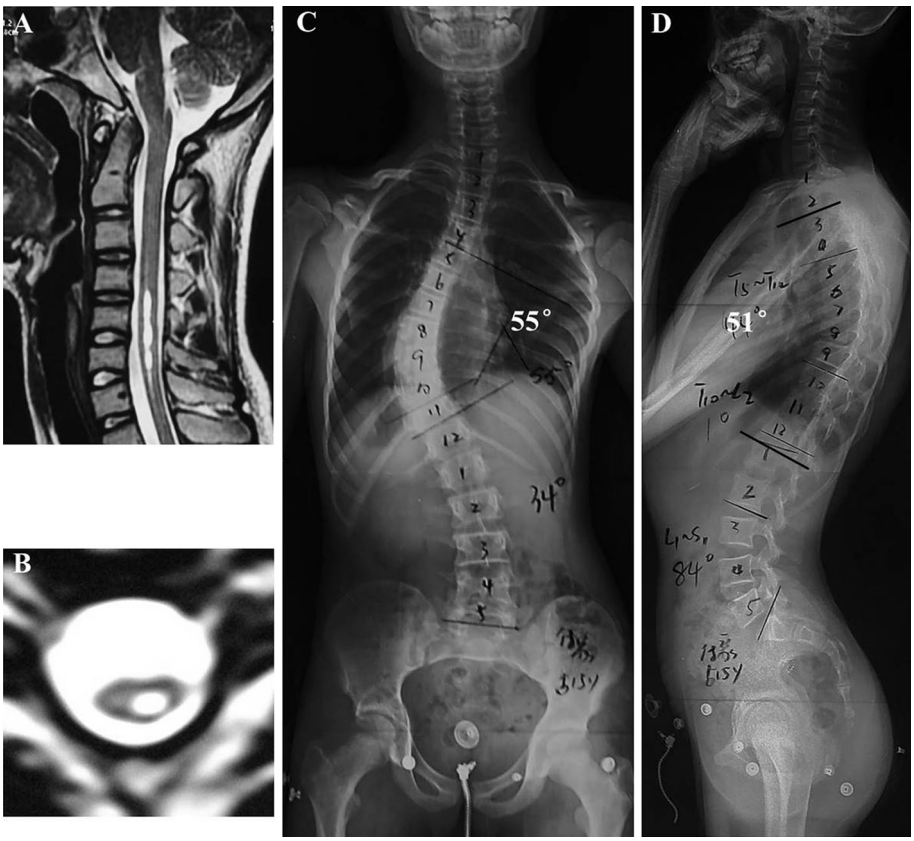

Fig. 2 A 15-year-old male with left thoracic scoliosis (**c**) secondary to idiopathic syringomyelia (**a**). The syrinx was observed to be deviated to the left on transverse MR images (**b**). Standing lateral radiograph (**d**) demonstrates a hyperkyphotic component of the thoracic spine (51°)

In light of these clinical and radiological similarities, CMI and IS are hypothesized to share a common pathophysiological mechanism implicating an underlying genetic or epigenetic component [4].

Scoliosis is commonly seen in both IS and CMI patients. To our knowledge, however, no study has directly compared the imaging features of spinal deformities between these two populations. In this series, radiographic

Table 3 Comparison of scoliosis features between idiopathic and Chiari I-type syringomyelia

Variable	Scoliosis secondary to IS	Scoliosis secondary to CMI-type syringomyelia		*P*
	Present study	Qiu et al. [31]	Spiegel et al. [5]	
Sample size	61	87	41	
Age (years)	15.5	12.9	12.1	
Primary curve magnitude (°)	71.8	57.6	43.2	
Atypical coronal curve patterns	25 (41.0 %)	38 (43.7 %)	21 (51.2 %)	NS
Single left thoracic	19 (31.1 %)	28 (32.2 %)	8 (19.5 %)	
Left thoracic/right lumbar	2 (3.3 %)	3 (3.4 %)	2 (4.9 %)	
Left thoracic/right thoracolumbar	0	0	1 (2.4 %)	
Double thoracic	3 (4.9 %)	6 (6.9 %)	4 (9.8 %)	
Right thoracic (King IV)	1 (1.6 %)	1 (1.1 %)	4 (9.8 %)	
Typical coronal curve patterns	36 (59.0 %)	49 (56.3 %)	20 (48.8 %)	NS
Single right thoracic	27 (44.2 %)	31 (35.6 %)	9 (22.0 %)	
Right thoracic/left lumbar	6 (9.8 %)	7 (8.0 %)	7 (17.1 %)	
Right thoracic/left thoracolumbar	0	1 (1.1 %)	2 (4.9 %)	
Lumbar/thoracolumbar	3 (4.9 %)	10 (11.5 %)	2 (4.9 %)	
Atypical feature in typical curve patterns	27 (75.0 %)	32 (65.3 %)	15 (75.0 %)	NS
Thoracic kyphosis				
Hyperkyphosis (>50°)	36.1 %	29.6 %	29 %	NS
Hypokyphosis (<20°)	4.9 %	2.5 %	5 %	
Normal (20°–50°)	59.0 %	67.9 %	66 %	
Lumbar lordosis				
Hyperlordosis (>74°)	14.8 %	11.1 %	24 %	NS
Hypolordosis (<54°)	42.6 %	49.4 %	24 %	
Normal (54°–74°)	42.6 %	39.5 %	52 %	

IS idiopathic syringomyelia, *CMI* Chiari I malformation, *NS* statistical non-significance

Table 4 Correlation between curve direction and the side of deviated syrinx in patients with single thoracic scoliosis

Curve direction	Syrinx deviation		
	Left	Center	Right
Left	7	11	1
Right	2	18	8

Fisher exact test, $P = .021$

parameters of scoliosis in IS including coronal curve patterns, sagittal profiles and the frequency of atypical features were found to be very similar to those reported for CMI-associated scoliosis (Table 3), suggesting that the mechanism by which syrinx leads to spinal deformity may also be analogous between idiopathic and CMI-type syringomyelia. When different, the anteroposterior size and vertical length of the syrinx tended to be smaller in IS as compared to the CMI cohorts. This disparity, although is of uncertain significance, indeed joins a list of other similarly unexplained phenomena (for instance, milder neurologic symptoms [4] and minimally altered cerebrospinal fluid hydrokinetics [20] in IS patients) and bears out the notion that IS and CMI may represent different parts of the disease spectrum with additional genetic and/or environmental factors contributing to the phenotypic variation [4].

The mechanism underlying the development of scoliosis secondary to syringomyelia remains incompletely understood, although pressure from an asymmetrically expanded syrinx is generally believed to be imparted to the lower motor neurons or the dorsomedial/ventromedial aspects of the gray matter, causing an imbalance of trunk musculature and thus predisposing to scoliosis [8, 9, 26]. In an attempt to test this theory, several studies have explored the correlation between curve direction and the side of syrinx deviation. Yeom et al. [11] reported that the curve convexity was on the same side as the syrinx in 15 of 18 (83 %) patients with a deviated syrinx. Likewise, in 14 children with CMI-associated syringomyelia, Isu et al. [12] found that the syrinx was eccentrically located on the axial section and shifted to the convex side of the primary curve in all cases. Lately, Zhu et al. [10] systematically evaluated the correlation of the coronal asymmetries between

tonsillar ectopia, syrinx location and scoliosis, demonstrating that the thoracic curve was convex to the dominant side of the asymmetrically displaced tonsils in 88.5 % of patients and to the side of deviated syrinx in 86.2 %. Whereas these studies brought to light an interesting phenomenon that may contribute to a better understanding of the association between syringomyelia and scoliosis, the asymmetric nature of tonsillar ectopia per se in patients with CMI might have potentially confounded their results. Concentrating on IS patients without hindbrain herniation, the current analysis (focused on single thoracic scoliosis so as to obviate the dilemma in deciding the convex side of double major curves) revealed a 83.3 % consistency in laterality between curve convexity and the eccentrically located syrinx (Table 4), which concurred with the concordance rate reported by Yeom et al. [11]. Taken together, these findings suggest that the curve convexity could be influenced by deviation of the syrinx, providing further support for the involvement of spinal cord dysfunction in the pathogenesis of syringomyelia-associated scoliosis [8]. It should be noted, however, that a substantial number of cases (up to 66 %) in this series were classified as having centrally located syrinx as per the definition described by Zhu et al. [10]. Conceivably, such morphology-based classification utilizing arbitrarily defined threshold may not be able to reflect precisely on whether the impingement on spinal cord caused by the syrinx is symmetrical or not. As evidenced by the experimental work from Zhu et al. [9], the positive rates of abnormal spreading and γ subunit expression of acetylcholine receptors were both higher on the convex side than on the concave side of the curve, indicating that imbalance of neuronal input of the paravertebral muscles could be present in patients with syringomyelia-related scoliosis.

Previous small series on the relationship between location of the scoliosis and syrinx have yielded inconsistent results. Among 14 children with CMI-associated scoliosis, Isu et al. [12] observed a difference between single and double curves with respect to the location of the syrinx on axial section, and the primary curve occurred in each group at the level where the biased syrinx was present. In stark contrast, a later study [11] on 20 pediatric and adult patients failed to reveal evidence linking the location of the syrinx to that of the primary curve. Magge et al. [2] recently also described 12 IS patients aged 19 years or less, showing no consistent pattern of the syrinx location relative to the spinal deformity. In our series, although a marginally significant correlation ($P = .066$) was found between the primary curve apex and the level of maximum syrinx expansion, expounding this spatial relationship was not clear-cut. As syringomyelia predominantly involves the cervicothoracic segment in which the cervical enlargement of the spinal cord resides [16, 27], one can speculate that the medial nuclear group is more susceptible to the impact of expanding syringes as compared to the lateral nuclear group. However, how and to what extent this compromised spinal cord function may contribute to the de novo formation of scoliosis is still unclear.

As in previously reported series [11], curve magnitude of the spinal deformity did not have a statistically significant influence upon neurological findings in our study. Also of note is the observation that symptoms (19.7 %; including nonspecific symptoms such as back pain which could be purely coincidental rather than a direct result of the syrinx) and/or moderate to severe neurological deficit (11.5 %) were present in merely a minority of patients, which gives credence to the idea that IS is generally an asymptomatic, benign pathology for which conservative management would suffice [2, 3, 28]. Furthermore, our findings correspond with those of other authors [15, 29] in that anteroposterior size and vertical extent of the syrinx were not proportional to the neurological deficit.

The present study involves the largest cohort so far dedicated to the evaluation of the neuroimaging features of IS, with particular emphasis on the coronal asymmetries between scoliosis and eccentrically located syrinx. As far as we can determine, this is also the only study to compare the radiographic characteristics of spinal deformity between the idiopathic and Chiari-type syringomyelia populations.

Limitations inherent to this work include the retrospective, cross-sectional design. Given that not all patients with scoliosis underwent routine MRI assessment in our center, the possible effect of enrollment bias should also be considered in any interpretation of these results. In addition, it should be noted that the term “IS” used in our study refers to a syrinx of unknown origin, with absence of an underlying pathology on MR scans and no history of a preexisting condition that may potentially lead to the formation of syringomyelia [2, 3, 28]. In this context, this term does not necessarily imply the absence of an underlying cause, but, rather, the absence of a cause that can be detected using standard diagnostic methods [21]. However, what should be considered the “standard” procedure for assessing syringomyelia will certainly change as the diagnostic technique evolves, and so will the definition for IS. Lately, several published studies [20, 21, 23, 30] demonstrated that abnormal cerebral spinal fluid (CSF) flow hydrodynamics has a key role in the pathogenesis of syringomyelia, irrespective of whether the syrinx presents as “idiopathic” or another form [31, 32]. This is particularly intriguing considering that some universal mechanism may underlie the development of all types of syrinx, as proposed by Greitz [31]. Due to the retrospective nature of this review, however, CSF circulation features were not evaluated in the patients recruited in this study. Moreover,

using dynamic MRI studies or high-resolution MRI protocol such as 3D-CISS sequence would make a more accurate and reliable assessment of their syringes.

Conclusions

Radiological characteristics of scoliosis were found to be similar between IS and CMI-type syringomyelia in both the coronal and sagittal planes, adding further evidence to the concept that these entities may share a common pathophysiological mechanism. The thoracic spine in IS patients tended to be convex to the deviated side of the eccentrically located syrinx, which indirectly supported the role of spinal cord dysfunction in the pathogenesis of syringomyelia-associated scoliosis.

Acknowledgments This work was supported by the National Natural Science Foundation of China (Grant No. 81371912).

Compliance with ethical standards

Conflict of interest No benefits in any form have been or will be received from a commercial party related directly or indirectly to the subject of this manuscript.

References

1. Milhorat TH, Chou MW, Trinidad EM, Kula RW, Mandell M, Wolpert C, Speer MC (1999) Chiari I malformation redefined: clinical and radiographic findings for 364 symptomatic patients. Neurosurgery 44:1005–1017
2. Magge SN, Smyth MD, Governale LS, Goumnerova L, Madsen J, Munro B, Nalbach SV, Proctor MR, Scott RM, Smith ER (2011) Idiopathic syrinx in the pediatric population: a combined center experience. J Neurosurg Pediatr 7:30–36
3. Joseph RN, Batty R, Raghavan A, Sinha S, Griffiths PD, Connolly DJA (2013) Management of isolated syringomyelia in the paediatric population—a review of imaging and follow-up in a single centre. Br J Neurosurg 27:683–686
4. Markunas CA, Tubbs RS, Moftakhar R, Ashley-Koch AE, Gregory SG, Oakes WJ, Speer MC, Iskandar BJ (2012) Clinical, radiological, and genetic similarities between patients with Chiari Type I and Type 0 malformations. J Neurosurg Pediatr 9:372–378
5. Spiegel DA, Flynn JM, Stasikelis PJ, Dormans JP, Drummond DS, Gabriel KR, Loder RT (2003) Scoliotic curve patterns in patients with Chiari I malformation and/or syringomyelia. Spine (Phila Pa 1976) 28:2139–2146
6. Qiu Y, Zhu Z, Wang B, Yu Y, Qian B, Zhu F (2008) Radiological presentations in relation to curve severity in scoliosis associated with syringomyelia. J Pediatr Orthop 28:128–133
7. Ouellet JA, LaPlaza J, Erickson MA, Birch JG, Burke S, Browne R (2003) Sagittal plane deformity in the thoracic spine: a clue to the presence of syringomyelia as a cause of scoliosis. Spine (Phila Pa 1976) 28:2147–2151
8. Huebert HT, MacKinnon WB (1969) Syringomyelia and scoliosis. J Bone Joint Surg (Br) 51:338–343
9. Zhu Z, Qiu Y, Wang B, Yu Y, Qian B, Zhu F (2007) Abnormal spreading and subunit expression of junctional acetylcholine receptors of paraspinal muscles in scoliosis associated with syringomyelia. Spine 32:2449–2454
10. Zhu Z, Wu T, Sha S, Sun X, Zhu F, Qian B, Qiu Y (2013) Is curve direction correlated with the dominant side of tonsillar ectopia and side of syrinx deviation in patients with single thoracic scoliosis secondary to Chiari malformation and syringomyelia? Spine (Phila Pa 1976) 38:671–677
11. Yeom JS, Lee CK, Park KW, Lee JH, Lee DH, Wang KC, Chang BS (2007) Scoliosis associated with syringomyelia: analysis of MRI and curve progression. Eur Spine J 16:1629–1635
12. Isu T, Chono Y, Iwasaki Y, Koyanagi I, Akino M, Abe H, Abumi K, Kaneda K (1992) Scoliosis associated with syringomyelia presenting in children. Childs Nerv Syst 8:97–100
13. Ono A, Ueyama K, Okada A, Echigoya N, Yokoyama T, Harata S (2002) Adult scoliosis in syringomyelia associated with Chiari I malformation. Spine (Phila Pa 1976) 27:E23–E28
14. AKarnofsky D, Burchenal JH (1949) The clinical evaluation of chemotherapeutic agents in cancer. In: MacLeod CM (ed) Evaluation of chemotherapeutic agents. Columbia University Press, New York, pp 191–205
15. Arnautovic KI, Muzevic D, Splavski B, Boop FA (2013) Association of increased body mass index with Chiari malformation Type I and syrinx formation in adults. J Neurosurg 119:1058–1067
16. Tokunaga M, Minami S, Isobe K, Moriya H, Kitahara H, Nakata Y (2001) Natural history of scoliosis in children with syringomyelia. J Bone Joint Surg Br 83:371–376
17. Boseker EH, Moe JH, Winter RB, Koop SE (2000) Determination of "normal" thoracic kyphosis: a roentgenographic study of 121 "normal" children. J Pediatr Orthop 20:796–798
18. Bernhardt M, Bridwell KH (1989) Segmental analysis of the sagittal plane alignment of the normal thoracic and lumbar spines and thoracolumbar junction. Spine (Phila Pa 1976) 14:717–721
19. Vedantam R, Lenke LG, Keeney JA, Bridwell KH (1998) Comparison of standing sagittal spinal alignment in asymptomatic adolescents and adults. Spine (Phila Pa 1976) 23:211–215
20. Struck AF, Haughton VM (2009) Idiopathic syringomyelia: phase-contrast MR of cerebrospinal fluid flow dynamics at level of foramen magnum. Radiology 253:184–190
21. Mauer UM, Freude G, Danz B, Kunz U (2008) Cardiac-gated phase-contrast magnetic resonance imaging of cerebrospinal fluid flow in the diagnosis of idiopathic syringomyelia. Neurosurgery 63:1139–1144
22. Hirano M, Haughton V, Munoz del Rio A (2012) Tapering of the cervical spinal canal in patients with Chiari I malformations. Am J Neuroradiol 33:1326–1330
23. Bogdanov EI, Heiss JD, Mendelevich EG, Mikhaylov IM, Haass A (2004) Clinical and neuroimaging features of "idiopathic" syringomyelia. Neurology 62:791–794
24. Chern JJ, Gordon AJ, Mortazavi MM, Tubbs RS, Oakes WJ (2011) Pediatric Chiari malformation Type 0: a 12-year institutional experience. J Neurosurg Pediatr 8:1–5
25. Kyoshima K, Kuroyanagi T, Oya F, Kamijo Y, El-Noamany H, Kobayashi S (2002) Syringomyelia without hindbrain herniation: tight cisterna magna. Report of four cases and a review of the literature. J Neurosurg 96:239–249
26. Batzdorf U, Khoo LT, McArthur DL (2007) Observations on spine deformity and syringomyelia. Neurosurgery 61:370–378
27. Ozerdemoglu R, Denis F, Transfeldt E (2003) Scoliosis associated with syringomyelia: clinical and radiologic correlation. Spine 28:1410–1417
28. Roy AK, Slimack NP, Ganju A (2011) Idiopathic syringomyelia: retrospective case series, comprehensive review, and update on management. Neurosurg Focus 31:E15

29. Alzate JC, Kothbauer KF, Jallo GI, Epstein FJ (2001) Treatment of Chiari I malformation in patients with and without syringomyelia: a consecutive series of 66 cases. Neurosurg Focus 11:E3
30. Heiss JD, Snyder K, Peterson MM, Patronas NJ, Butman JA, Smith RK, DeVroom HL, Sansur CA, Eskioglu E, Kammerer WA, Oldfield EH (2012) Pathophysiology of primary spinal syringomyelia. J Neurosurg Spine 17:367–380
31. Greitz D (2006) Unraveling the riddle of syringomyelia. Neurosurg Rev 29:251–264
32. Klekamp J (2002) The pathophysiology of syringomyelia—historical overview and current concept. Acta Neurochir (Wien) 144:649–664